
Understanding Black-box Predictions via Influence Functions

Pang Wei Koh¹ Percy Liang¹

Abstract

How can we explain the predictions of a black-box model? In this paper, we use influence functions — a classic technique from robust statistics — to trace a model’s prediction through the learning algorithm and back to its training data, identifying the points most responsible for a given prediction. Applying ideas from second-order optimization, we scale up influence functions to modern machine learning settings and show that they can be applied to high-dimensional black-box models, even in non-convex and non-differentiable settings. We give a simple, efficient implementation that requires only oracle access to gradients and Hessian-vector products. On linear models and convolutional neural networks, we demonstrate that influence functions are useful for many different purposes: to understand model behavior, debug models and detect dataset errors, and even identify and exploit vulnerabilities to adversarial training-set attacks.

1. Introduction

A key question often asked of machine learning systems is “Why did the system make this prediction?” We want models that are not just high-performing but also explainable. By understanding why a model does what it does, we can hope to improve the model (Amershi et al., 2015), discover new science (Shrikumar et al., 2016), and provide end-users with explanations of actions that impact them (Goodman & Flaxman, 2016).

However, the best-performing models in many domains — e.g., deep neural networks for image and speech recognition (Krizhevsky et al., 2012) — are complicated, black-box models whose predictions seem hard to explain. Work on interpreting these black-box models has focused on understanding how a given model leads to particular predictions, e.g., by locally fitting a simpler model around the test point (Ribeiro et al., 2016) or by perturbing the test point to see how the prediction changes (Simonyan et al., 2013; Li

et al., 2016b; Datta et al., 2016; Adler et al., 2016). These works explain the predictions in terms of the model, but how can we explain where the model came from?

In this paper, we tackle this question by tracing a model’s predictions through its learning algorithm and back to its training data, where the model parameters ultimately derive from. To formalize the impact on a training point on a prediction, we ask the counterfactual: what would happen if we did not have this training point, or if the values of this training point were changed slightly?

Answering this question by perturbing the data and retraining the model can be prohibitively expensive. To overcome this problem, we use influence functions, a classic technique from robust statistics (Cook & Weisberg, 1980) that tells us how the model parameters change as we upweight a training point by an infinitesimal amount. With these, we can “differentiate through the training” to estimate in closed-form the effect of a variety of training perturbations.

Despite their rich history in statistics, influence functions have not seen widespread use in machine learning; to the best of our knowledge, the work closest to ours is a recent paper from Wojnowicz et al. (2016), which introduced a method for approximating Cook’s distance (a quantity related to influence) in generalized linear models. One obstacle to adoption is that influence functions require expensive second derivative calculations and assume differentiability and convexity of the model, limiting their applicability in modern contexts where models are often non-differentiable, non-convex, and high-dimensional.

We address this challenge by efficiently approximating influence functions using techniques from second-order optimization (Pearlmutter, 1994; Martens, 2010; Agarwal et al., 2016). We also demonstrate that influence functions can remain accurate even as their underlying assumptions of differentiability and convexity degrade.

Influence functions capture the core idea of studying models through the lens of their training data. We show that they are a versatile tool that can be applied to a wide variety of seemingly disparate tasks: understanding model behavior; debugging models; detecting dataset errors; and creating visually-indistinguishable adversarial *training* examples that can flip neural network test predictions, the training set analogue of Goodfellow et al. (2015).

¹Stanford University, Stanford, CA. Correspondence to: Pang Wei Koh <pangwei@cs.stanford.edu>, Percy Liang <плиang@cs.stanford.edu>. Copyright 2017 by the author(s).

2. Approach

2.1. Changing the weight of a training point

Our goal is to understand the effect of training points on a model’s predictions. We formalize this goal by asking the counterfactual: how would the model’s predictions change if we did not have this training point?

Consider an unconstrained empirical risk minimization setting, i.e., the parameters $\hat{\theta} \triangleq \arg \min_{\theta \in \Theta} \frac{1}{n} \sum_{i=1}^n L(z_i, \theta)$ minimize some loss function L over training data z_1, \dots, z_n , where $z_i = (x_i, y_i) \in \mathcal{X} \times \mathcal{Y}$ and we fold in regularization terms into L . Assume that the empirical risk $\frac{1}{n} \sum_{i=1}^n L(z_i, \theta)$ is twice-differentiable and strongly convex in θ in a local neighborhood around $\hat{\theta}$, i.e., the Hessian $H_{\hat{\theta}} = \frac{1}{n} \sum_{i=1}^n \nabla_{\theta}^2 L(z_i, \hat{\theta})$ exists and is positive definite (PD); in section 4 we explore relaxing these assumptions.

We wish to compute $\hat{\theta}_{-z} - \hat{\theta}$ for all training points z , where $\hat{\theta}_{-z} \triangleq \arg \min_{\theta \in \Theta} \sum_{z_i \neq z} L(z_i, \theta)$; this is the change in the model parameters when z is removed. However, retraining the model for each removed z is prohibitively slow.

Fortunately, influence functions give us an efficient approximation. The idea is to compute the parameter change if z were upweighted by some small ϵ , giving us new parameters $\hat{\theta}_{\epsilon, z} \triangleq \arg \min_{\theta \in \Theta} (1 - \epsilon) \frac{1}{n} \sum_{i=1}^n L(z_i, \theta) + \epsilon L(z, \theta)$. A classic result (Cook & Weisberg, 1982) tells us that the influence of upweighting z on the parameters $\hat{\theta}$ is given by

$$\mathcal{I}_{\text{up, params}}(z) \triangleq \left. \frac{d\hat{\theta}_{\epsilon, z}}{d\epsilon} \right|_{\epsilon=0} = -H_{\hat{\theta}}^{-1} \nabla_{\theta} L(z, \hat{\theta}).x \quad (1)$$

In essence, we form a quadratic approximation to the empirical risk around $\hat{\theta}$ and take a single Newton step; see appendix A for a derivation. Since removing a point is the same as removing $\frac{1}{n}$ weight from it, we can make the linear approximation $\hat{\theta}_{-z} - \hat{\theta} \approx -\frac{1}{n} \mathcal{I}_{\text{up, params}}(z)$ without retraining the model.

We can apply the chain rule to measure how upweighting z changes functions of $\hat{\theta}$. In particular, the influence of upweighting z on the loss at a test point z_{test} is

$$\begin{aligned} \mathcal{I}_{\text{up, loss}}(z, z_{\text{test}}) &\triangleq \left. \frac{dL(z_{\text{test}}, \hat{\theta}_{\epsilon, z})}{d\epsilon} \right|_{\epsilon=0} \\ &= \nabla_{\theta} L(z_{\text{test}}, \hat{\theta})^{\top} \left. \frac{d\hat{\theta}_{\epsilon, z}}{d\epsilon} \right|_{\epsilon=0} \\ &= -\nabla_{\theta} L(z_{\text{test}}, \hat{\theta})^{\top} H_{\hat{\theta}}^{-1} \nabla_{\theta} L(z, \hat{\theta}). \end{aligned} \quad (2)$$

2.2. Perturbing the training input

We can develop a finer-grained notion of influence by studying a different counterfactual: how would the model’s predictions change if a training input were modified?

Let $z = (x, y)$ be some training point and $z_{\delta} \triangleq (x + \delta, y)$.

Consider the perturbation $z \mapsto z_{\delta}$, and let the resulting parameters be $\hat{\theta}_{z_{\delta}, -z}$. We can interpret this perturbation as removing $\frac{1}{n}$ weight from z and adding it to a new “phantom” point z_{δ} . To approximate its effects, consider moving infinitesimal ϵ weight from z onto z_{δ} . Letting the resulting parameters be $\hat{\theta}_{\epsilon, z_{\delta}, -z}$, eqn 1 gives us

$$\begin{aligned} \left. \frac{d\hat{\theta}_{\epsilon, z_{\delta}, -z}}{d\epsilon} \right|_{\epsilon=0} &= \mathcal{I}_{\text{up, params}}(z_{\delta}) - \mathcal{I}_{\text{up, params}}(z) \\ &= -H_{\hat{\theta}}^{-1} (\nabla_{\theta} L(z_{\delta}, \hat{\theta}) - \nabla_{\theta} L(z, \hat{\theta})). \end{aligned} \quad (3)$$

As before, we can make the linear approximation $\hat{\theta}_{z_{\delta}, -z} - \hat{\theta} \approx \left. \frac{d\hat{\theta}_{\epsilon, z_{\delta}, -z}}{d\epsilon} \right|_{\epsilon=0} \cdot \frac{1}{n}$, giving us a closed-form estimate of the effect of $z \mapsto z_{\delta}$ on the model. Analogous equations also apply for changes in y . While influence functions might appear to only work for infinitesimal (therefore continuous) perturbations, it is important to note that this approximation holds for arbitrary δ : the ϵ -upweighting scheme allows us to smoothly interpolate between z and z_{δ} . This is particularly useful for working with discrete data (e.g., in NLP) or with discrete label changes.

If x is continuous and δ is small, we can further approximate eqn 3. Assume that the input domain $\mathcal{X} \subseteq \mathbb{R}^d$, the parameters $\Theta \subseteq \mathbb{R}^p$, and L is differentiable in θ and x . As $\|\delta\| \rightarrow 0$, $\nabla_{\theta} L(z_{\delta}, \hat{\theta}) - \nabla_{\theta} L(z, \hat{\theta}) \approx [\nabla_x \nabla_{\theta} L(z, \hat{\theta})] \delta$, where $\nabla_x \nabla_{\theta} L(z, \hat{\theta}) \in \mathbb{R}^{p \times d}$. Substituting into eqn 3,

$$\left. \frac{d\hat{\theta}_{\epsilon, z_{\delta}, -z}}{d\epsilon} \right|_{\epsilon=0} = -H_{\hat{\theta}}^{-1} [\nabla_x \nabla_{\theta} L(z, \hat{\theta})] \delta. \quad (4)$$

We thus have $\hat{\theta}_{z_{\delta}, -z} - \hat{\theta} \approx -\frac{1}{n} H_{\hat{\theta}}^{-1} [\nabla_x \nabla_{\theta} L(z, \hat{\theta})] \delta$. Differentiating w.r.t. δ and applying the chain rule gives us

$$\begin{aligned} \mathcal{I}_{\text{pert, loss}}(z, z_{\text{test}}) &\triangleq \left. \nabla_{\delta} L(z_{\text{test}}, \hat{\theta}_{z_{\delta}, -z}) \right|_{\delta=0} \\ &= -\nabla_{\theta} L(z_{\text{test}}, \hat{\theta})^{\top} H_{\hat{\theta}}^{-1} \nabla_x \nabla_{\theta} L(z, \hat{\theta}). \end{aligned} \quad (5)$$

$[\mathcal{I}_{\text{pert, loss}}(z, z_{\text{test}})] \delta$ tells us the approximate effect that $z \mapsto z + \delta$ has on the loss at z_{test} . By setting δ in the direction of $\mathcal{I}_{\text{pert, loss}}(z, z_{\text{test}})$, we can construct local perturbations of z that maximally increase the loss at z_{test} . In section 5.2, we will use this to construct dataset poisoning attacks.

$\mathcal{I}_{\text{pert, loss}}$ also appears when identifying the features responsible for the influence of z on z_{test} . One way to do this is to pick the largest components of $\nabla_x \mathcal{I}_{\text{up, loss}}(z, z_{\text{test}})$, i.e., the features that most change influence when perturbed. Comparing eqns 2 and 5, we see that $\nabla_x \mathcal{I}_{\text{up, loss}}(z, z_{\text{test}}) \approx \mathcal{I}_{\text{pert, loss}}(z, z_{\text{test}})$ up to an $O(\frac{1}{n})$ term (since $H_{\hat{\theta}} = \frac{1}{n} \sum_i \nabla_{\theta}^2 L(z_i, \hat{\theta})$ depends on z).

2.3. Relation to Euclidean distance

To find the training examples most relevant to a test example, it is common to look at its nearest neighbors in Euclidean space (e.g., Ribeiro et al. (2016)); with normalized

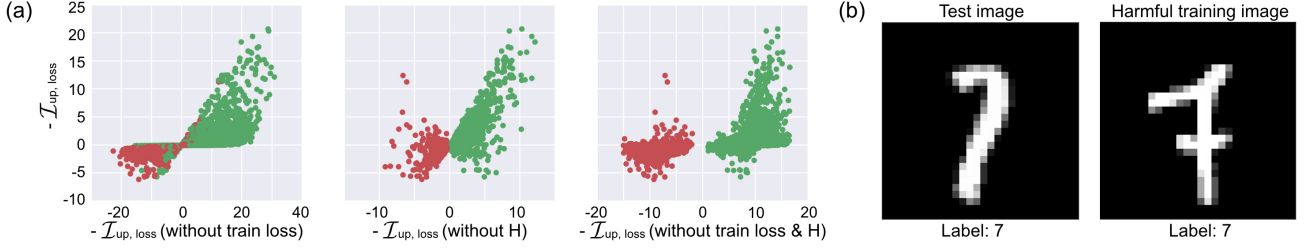


Figure 1. Influence functions vs. Euclidean inner product. (a) Compared to $\mathcal{I}_{\text{up,loss}}$, the inner product is missing two key terms, train loss and $H_{\hat{\theta}}$. Here, we plot $\mathcal{I}_{\text{up,loss}}$ against variants that are missing these terms and show that they are necessary for picking up the truly influential training points. These results are from a logistic regression model trained to distinguish 1’s from 7’s in MNIST (LeCun et al., 1998). We picked an arbitrary test point z_{test} ; similar trends hold across other test points. Green dots are train images of the same label as the test image (7) while red dots are 1’s. **Left:** Without the train loss term, we overestimate the influence of many training points (e.g., the points on the y-axis should have $\mathcal{I}_{\text{up,loss}}$ close to 0, but instead have high influence when we remove the train loss term). **Mid:** Without $H_{\hat{\theta}}$, all green points are helpful (to the right of the line at $x=0$) and all red points are harmful. This is because $\forall x, x \succeq 0$ (all pixel values are positive), so $x \cdot x_{\text{test}} \geq 0$, but it is incorrect: many harmful training points actually share the same label as z_{test} . See panel (b). **Right:** Without training loss or $H_{\hat{\theta}}$, what is left is essentially the Euclidean inner product, which fails to accurately capture influence; the scatter plot deviates quite far from the $y=x$ line. (b) The test image and a harmful training image with the same label. To the model, they look very different, so the presence of the training image makes the model think that the test image is less likely to be a 7. The Euclidean inner product does not pick up on these less intuitive, but important, harmful influences.

vectors, this is equivalent to choosing x with large $x \cdot x_{\text{test}}$. For intuition, we compare this to $\mathcal{I}_{\text{up,loss}}(z, z_{\text{test}})$ on a logistic regression model and show that influence is much more accurate at accounting for the effect of training.

Let $p(y | x) = \sigma(y\theta^\top x)$, with $y \in \{-1, 1\}$ and $\sigma(t) = \frac{1}{1+\exp(-t)}$. We seek to maximize the probability of the training set. For a training point $z = (x, y)$, $L(z, \theta) = \log(1 + \exp(-y\theta^\top x))$, $\nabla_{\theta} L(z, \theta) = -\sigma(-y\theta^\top x)yx$, and $H_{\theta} = \frac{1}{n} \sum_{i=1}^n \sigma(\theta^\top x_i) \sigma(-\theta^\top x_i) x_i x_i^\top$. From eqn 2, $\mathcal{I}_{\text{up,loss}}(z, z_{\text{test}})$ is:

$$-y_{\text{test}} y \cdot \sigma(-y_{\text{test}} \theta^\top x_{\text{test}}) \cdot \sigma(-y \theta^\top x_k) \cdot x_{\text{test}}^\top H_{\hat{\theta}}^{-1} x.$$

We highlight two key differences from $x \cdot x_{\text{test}}$. First, $\sigma(-y\theta^\top x)$ gives points with high training loss more influence, revealing that outliers can dominate the model parameters. Second, the weighted covariance matrix $H_{\hat{\theta}}^{-1}$ measures the “resistance” of the other training points to the removal of z ; if $\nabla_{\theta} L(z, \hat{\theta})$ points in a direction where there is little variation, its influence will be higher since moving in that direction will not significantly increase the loss on other training points. As we show in Fig 1, these differences mean that influence functions capture the effect of model training much more accurately.

3. Efficiently calculating influence

There are two challenges to efficiently computing $\mathcal{I}_{\text{up,loss}}(z, z_{\text{test}}) = -\nabla_{\theta} L(z_{\text{test}}, \hat{\theta})^\top H_{\hat{\theta}}^{-1} \nabla_{\theta} L(z, \hat{\theta})$. First, it requires forming and inverting $H_{\hat{\theta}} = \frac{1}{n} \sum_{i=1}^n \nabla_{\theta}^2 L(z_i, \hat{\theta})$, the Hessian of the empirical risk. With n training points and $\theta \in \mathbb{R}^p$, this requires $O(np^2 + p^3)$ operations, which

can be prohibitively expensive in models like deep neural networks with millions of parameters. Second, in a typical application we are not just interested in a single pair of (z, z_{test}) ; instead, we might want to calculate $\mathcal{I}_{\text{up,loss}}(z_i, z_{\text{test}})$ across all training points z_i and a few test points of interest z_{test} .

The first problem is well-studied in second-order optimization. The idea is to avoid explicitly evaluating $H_{\hat{\theta}}^{-1}$; instead, we use implicit Hessian-vector products (HVPs) to efficiently approximate $s_{\text{test}} \triangleq H_{\hat{\theta}}^{-1} \nabla_{\theta} L(z_{\text{test}}, \hat{\theta})$ and then compute $\mathcal{I}_{\text{up,loss}}(z, z_{\text{test}}) = -s_{\text{test}} \cdot \nabla_{\theta} L(z, \hat{\theta})$. This also gives a solution to the second problem: if we have a few test points of interest, we can precompute s_{test} for each of them and then efficiently compute $-s_{\text{test}} \cdot \nabla_{\theta} L(z_i, \hat{\theta})$ for all training points z_i .

We discuss two techniques for approximating s_{test} , both relying on the fact that the HVP of a single term in $H_{\hat{\theta}}$, $[\nabla_{\theta}^2 L(z_i, \hat{\theta})]v$, can be computed for arbitrary v in roughly the same amount of time that $\nabla_{\theta} L(z_i, \hat{\theta})$ would take, which is typically $O(p)$ (Pearlmutter, 1994). These HVPs can be computed via auto-differentiation: the idea is to calculate $\nabla_{\theta} L(z_i, \hat{\theta})$ with one pass, symbolically form $\nabla_{\theta} L(z_i, \hat{\theta}) \cdot v$, and then differentiate it to get $\nabla_{\theta} (\nabla_{\theta} L(z_i, \hat{\theta}) \cdot v) = [\nabla_{\theta}^2 L(z_i, \hat{\theta})]v$.

Conjugate gradients (CG). The first technique is a standard transformation of matrix inversion into an optimization problem. Since $H_{\hat{\theta}} \succ 0$ by assumption, $H_{\hat{\theta}}^{-1}v \equiv \arg \min_t \{t^\top H_{\hat{\theta}} t - v^\top t\}$. We can solve this with CG approaches that only require the evaluation of $H_{\hat{\theta}} t$, which takes $O(np)$ time, without explicitly forming $H_{\hat{\theta}}$. While an

exact solution takes p CG iterations, in practice we can get a good approximation with fewer iterations; see [Martens \(2010\)](#) for more details.

Stochastic estimation. With large datasets, standard CG can be slow; each iteration still goes through all n training examples. We use a method developed by [Agarwal et al. \(2016\)](#) to get a stochastic estimator that only samples a single point per iteration, achieving a significant speedup.

Dropping the $\hat{\theta}$ subscript for clarity, let $H_j^{-1} = \sum_{i=0}^j (I - H)^i$, the first j terms in the Taylor expansion of H^{-1} . Rewrite this recursively as $H_j^{-1} = I + (I - H)H_{j-1}^{-1}$. From the validity of the Taylor expansion, $H_j^{-1} \rightarrow H^{-1}$ as $j \rightarrow \infty$.¹ The key is that at each iteration, we can substitute the full H with a draw from any unbiased (and faster-to-compute) estimator of H to form \tilde{H}_j . Since $\mathbb{E}[\tilde{H}_j^{-1}] = H_j^{-1}$, we still have $\mathbb{E}[\tilde{H}_j^{-1}] \rightarrow H^{-1}$.

In particular, we can use $\nabla_{\hat{\theta}}^2 L(z_i, \hat{\theta})$, for any z_i , as an unbiased estimator of H . This gives us the following procedure: uniformly sample t points z_{s_1}, \dots, z_{s_t} from the training data; define $\tilde{H}_0^{-1}v = v$; and recursively compute $\tilde{H}_j^{-1}v = v + (I - \nabla_{\hat{\theta}}^2 L(z_{s_j}, \hat{\theta}))\tilde{H}_{j-1}^{-1}v$, taking $\tilde{H}_t^{-1}v$ as our final unbiased estimate of $H^{-1}v$. We pick t to be large enough such that \tilde{H}_t stabilizes, and to reduce variance, we repeat this procedure r times and average results. Altogether, this is often significantly faster than CG.

We note that the original method of [Agarwal et al. \(2016\)](#) dealt only with generalized linear models, for which $[\nabla_{\hat{\theta}}^2 L(z_i, \hat{\theta})]v$ can be decomposed into two rank-one matrix-vector products that can be efficiently computed in $O(p)$ time. In our case, we rely on [Pearlmutter \(1994\)](#)'s more general algorithm for fast HVPs, described above, to achieve the same time complexity.²

With these techniques, we can compute $\mathcal{I}_{\text{up,loss}}(z_i, z_{\text{test}})$ on all training points z_i in $O(np + rtp)$ time; we show in section 4.1 that we can choose $rt < n$ and still have accurate results. Similarly, we can compute $\mathcal{I}_{\text{pert,loss}}(z_i, z_{\text{test}}) = -\frac{1}{n} \nabla_{\hat{\theta}} L(z_{\text{test}}, \hat{\theta})^\top H_{\hat{\theta}}^{-1} \nabla_x \nabla_{\hat{\theta}} L(z_i, \hat{\theta})$ with two matrix-vector products: we first compute s_{test} ,

¹We assume w.l.o.g. that $\forall i, \nabla_{\hat{\theta}}^2 L(z_i, \hat{\theta}) \preceq I$; if this is not true, we can scale the loss down without affecting the parameters. In some cases, we can get an upper bound on $\nabla_{\hat{\theta}}^2 L(z_i, \hat{\theta})$ (e.g., for linear models and bounded input), which makes this easy. Otherwise, we treat the scaling as a separate hyperparameter and tune it such that the Taylor expansion converges.

²One caveat of moving away from linear models is that we might not have $\nabla_{\hat{\theta}}^2 L(z, \hat{\theta}) \succ 0$ even if $H_{\hat{\theta}} \succ 0$, which may cause the recursive estimation of \tilde{H}_j to diverge. To get around this, we can add a small λI damping term to $\nabla_{\hat{\theta}}^2 L(z, \hat{\theta})$ and also average $\nabla_{\hat{\theta}}^2 L(z, \hat{\theta})$ over mini-batches of training points at each recursive step, instead of relying on a single training point. Empirically, this seems to give accurate results.

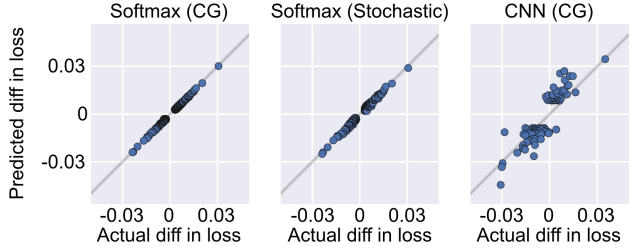


Figure 2. Influence vs. leave-one-out retraining. We arbitrarily picked one wrongly-classified test point z_{test} , but this trend held more broadly. These results are from 10-class MNIST. **Left:** For each of the 500 training points z with largest influence $|\mathcal{I}_{\text{up,loss}}(z, z_{\text{test}})|$, we plotted $-\frac{1}{n} \cdot \mathcal{I}_{\text{up,loss}}(z, z_{\text{test}})$ against the actual change in test loss after removing that point and retraining. The inverse HVP was solved exactly with CG. **Mid:** The same plot, but with the stochastic estimator. **Right:** The same plot for a CNN, computed on the 100 most influential points. For the actual difference in loss, we removed each point and retrained from $\hat{\theta}$ for 30k steps.

then find $s_{\text{test}}^\top \nabla_x \nabla_{\hat{\theta}} L(z_i, \hat{\theta})$ with the same HVP trick.

These computations are easy to implement in auto-grad systems like TensorFlow ([Abadi et al., 2015](#)) and Theano ([Theano D. Team, 2016](#)), as users need only specify the loss; the fast HVPs and the required gradients are automatically handled with minimal human effort. We will release code that works for models already defined in TensorFlow (as well as code to replicate the experiments in this paper).

4. Validation and extensions

Recall that influence functions are asymptotic approximations of leave-one-out retraining, and further, the approximations are only valid in theory when (i) the model parameters $\hat{\theta}$ minimize the empirical risk, and that (ii) the empirical risk is twice-differentiable and strongly convex in a local neighborhood around $\hat{\theta}$. In this section, we empirically show that influence functions are accurate approximations (section 4.1) and that they provide useful information even when these assumptions are violated (sections 4.2, 4.3).

4.1. Influence functions vs. leave-one-out retraining

Influence functions assume that the weight on a training point is changed by an infinitesimally small ϵ . To investigate the accuracy of influence functions when $\epsilon = \frac{1}{n}$, i.e., when we remove a training point and retrain the model, we compared $-\frac{1}{n} \mathcal{I}_{\text{up,loss}}(z, z_{\text{test}})$ with actually doing leave-one-out retraining ($\hat{\theta}_{-z} - \hat{\theta}$). With a softmax model on 10-class MNIST,³ the predicted and actual changes matched closely (Fig 2-Left).

³We trained with L-BFGS ([Liu & Nocedal, 1989](#)), with weight decay of 0.01, $n = 55,000$, and $p = 7,840$ parameters.

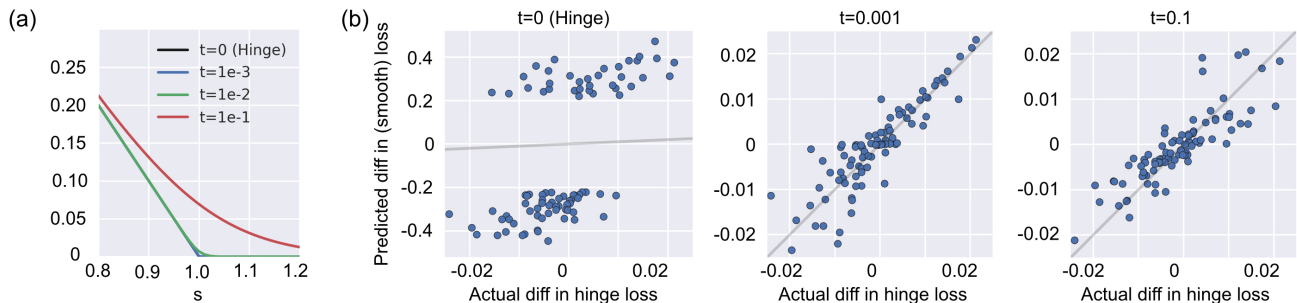


Figure 3. Smooth approximations to the hinge loss. (a) By varying t , we can approximate the hinge loss with arbitrary accuracy: the black and blue lines are overlaid on top of each other. (b) Using a random, wrongly-classified test point, we compared the predicted vs. actual differences in loss after leave-one-out retraining on the 100 most influential training points. A similar trend held for other test points. The SVM objective is to minimize $0.01 \|w\|_2^2 + \frac{1}{n} \sum_i \text{Hinge}(w^\top x_i)$. **Left:** Influence functions were unable to accurately predict the change, overestimating its magnitude considerably. **Mid:** Using $\text{SmoothHinge}(\cdot, 0.001)$ let us accurately predict the change in the hinge loss after retraining. **Right:** Correlation remained high over a wide range of t , though it degraded when t was too large. When $t = 1e-4$, Pearson R = 0.94; when $t = 1e-1$, Pearson R = 0.91.

The stochastic estimator was also accurate with $r = 10$ repeats and $t = 5,000$ iterations (Fig 2-Mid). Since each iteration only requires one HVP $[\nabla_\theta^2 L(z_i, \hat{\theta})]v$, this runs quickly: in fact, we accurately estimated $H^{-1}v$ without even looking at every data point, since in this case $n = 55,000 > rt$. Surprisingly, even setting $r = 1$ worked; it gave noisier but correlated results and was quite accurate at finding the most influential points.

4.2. Non-convexity and non-convergence

In section 2, we took $\hat{\theta}$ as the global minimum. In practice, if we obtain our model parameters $\tilde{\theta}$ through methods like SGD, we are not guaranteed that $\tilde{\theta} = \hat{\theta}$. Non-convexity could trap us in a local minimum; or if the model has not converged, $\tilde{\theta}$ might not be a local minimum and $H_{\tilde{\theta}}$ could have negative eigenvalues. We show that influence functions applied to $\tilde{\theta}$ still give meaningful results in practice.

If $\tilde{\theta}$ is a local minimum, $L(z, \cdot)$ is still approximately quadratic around $L(z, \tilde{\theta})$. As such, influence functions are locally meaningful: they tell us what happens if we up-weight a training point z and retrain with gradient descent starting from $\tilde{\theta}$, i.e., staying at the “same” local minimum.

If $\tilde{\theta}$ is close to a local minimum and $H_{\tilde{\theta}} \succ 0$, $\mathcal{I}_{\text{up,params}}(z)$ is correlated with the result of taking a single Newton step from $\tilde{\theta}$ after removing ϵ weight from z (see appendix B for a more precise statement). If $H_{\tilde{\theta}}$ has non-positive eigenvalues, the Newton step is not well-defined. We can add a small damping term λI to $H_{\tilde{\theta}}$ to control the negative curvature and make $H_{\tilde{\theta}} \succ 0$; this has the effect of regularizing the new $\tilde{\theta}_{\epsilon,z}$ to be near the original $\tilde{\theta}$.⁴

⁴In practice, we can efficiently find the smallest eigenvalue of $H_{\tilde{\theta}}$ through methods like power iteration, which rely only on HVPs, and use this to set the amount of damping.

We checked the behavior of $\mathcal{I}_{\text{up,loss}}$ in a non-convergent, non-convex setting by training a convolutional neural network for 500k iterations.⁵ The model had not converged and $H_{\tilde{\theta}}$ was not PD, so we added damping of $0.01I$. Even in this difficult setting, the predicted and actual changes in loss were highly correlated (Pearson R = 0.90, Fig 2-Right).

4.3. Non-differentiable losses

What happens when the derivatives of the loss, $\nabla_\theta L$ and $\nabla_\theta^2 L$, do not exist? In this section, we show that influence functions computed on smooth approximations to non-differentiable losses can predict the behavior of the original, non-differentiable loss under leave-one-out retraining. The robustness of this approximation suggests that we can train non-differentiable models and swap out non-differentiable components for smoothed versions for the purposes of calculating influence.

To see this, we trained a linear SVM on the same 1s vs. 7s MNIST task in section 2.3. This involves minimizing $\text{Hinge}(s) = \max(0, 1-s)$; this simple piecewise linear function is similar to ReLUs in neural networks, the most common source of their non-differentiability. We set the derivatives at the hinge to 0 and calculated $\mathcal{I}_{\text{up,loss}}$. As one might expect, this was inaccurate (Fig 3b-Left): because the second derivative is 0 everywhere except for regularization, $\mathcal{I}_{\text{up,loss}}$ overestimates how much it can move the pa-

⁵The network had 7 sets of convolutional layers with $\tanh(\cdot)$ non-linearities, modeled after the all-convolutional network from (Springenberg et al., 2014). For speed, we used 10% of the MNIST training set and only 2,616 parameters, since repeatedly retraining the network was expensive. Training was done with mini-batches of 500 examples and the Adam optimizer (Kingma & Ba, 2014). The model had not converged after 500k iterations; training it for another 500k iterations, using a full training pass for each iteration, reduced train loss from 0.146 to 0.120.

rameters and ends up predicting changes that are too large.

We approximated $\text{Hinge}(s)$ with $\text{SmoothHinge}(s, t) = t \log(1 + \exp(\frac{1-s}{t}))$, which approaches the hinge loss as $t \rightarrow 0$ (Fig 3a). Using the same SVM weights, we found that calculating $\mathcal{I}_{\text{up,loss}}$ using $\text{SmoothHinge}(s, 0.001)$ closely matched the predicted change in the original $\text{Hinge}(s)$ (Pearson R = 0.95; Fig 3b-Mid) and remained accurate over a wide range of t (Fig 3b-Right).

5. Use cases of influence functions

5.1. Understanding model behavior

By telling us the training points “responsible” for a given prediction, influence functions reveal insights about how models rely on and extrapolate from the training data. In this section, we show that two models can make the same correct predictions but get there in very different ways.

We compared (a) the state-of-the-art Inception v3 network (Szegedy et al., 2016) with all but the top layer frozen⁶ and (b) an RBF SVM on a dog vs. fish image classification dataset we built from ImageNet (Russakovsky et al., 2015), with 900 training examples for each class. Freezing neural networks in this way is not uncommon in computer vision applications and is equivalent to training a softmax on the bottleneck features (Donahue et al., 2014). We picked a test image that both models got correct (Fig 4-Top) and used $\text{SmoothHinge}(\cdot, 0.001)$ for the SVM’s influence.

As expected, $\mathcal{I}_{\text{up,loss}}$ in the RBF SVM varied inversely with distance, with training images far from the test image in pixel space having almost no influence; the Inception influences were much less correlated with distance in pixel space (Fig 4-Left). Looking at the two most helpful images (most positive $-\mathcal{I}_{\text{up,loss}}$) for each model in Fig 4-Right, we see that the Inception network picked on the distinctive characteristics of clownfish, whereas the RBF SVM pattern matched against training images close in pixel space.

Moreover, in the RBF SVM, fish (green points) close to the test image were mostly helpful, while dogs (red) were mostly harmful, with the RBF acting as a soft nearest neighbor function (Fig 4-Left). In contrast, in the Inception network, fish and dogs could be both helpful and harmful for correctly classifying the test image as a fish; in fact, the 5th most helpful training image was a dog that, to the model, looked very different from the test fish (Fig 4-Top).

5.2. Adversarial training examples

In this section, we show that models that place a lot of influence on a small number of points can be surprisingly vulnerable to training input perturbations, posing a serious

⁶We used pre-trained weights from Keras (Chollet, 2015).

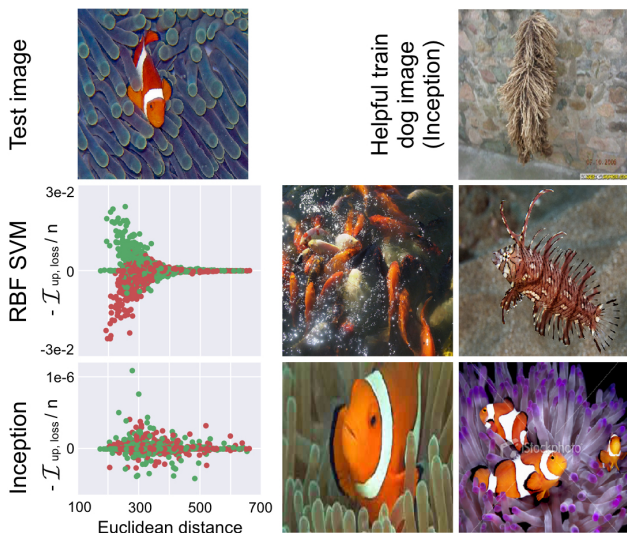


Figure 4. **Inception vs. RBF SVM.** **Bottom left:** $-\mathcal{I}_{\text{up,loss}}(z, z_{\text{test}})$ vs. $\|z - z_{\text{test}}\|_2^2$. Green dots are fish and red dots are dogs. **Bottom right:** The two most helpful training images, for each model, on the test. **Top right:** An image of a dog in the training set that helped the Inception model correctly classify the test image as a fish.

security risk in real-world ML systems where attackers can influence the training data (Huang et al., 2011). Recent work has generated adversarial *test* images that are visually indistinguishable from real test images but completely fool a classifier (Goodfellow et al., 2015). We demonstrate that influence functions can be used to craft adversarial *training* images that are similarly visually-indistinguishable and can flip a model’s prediction on a separate test image. To the best of our knowledge, this is the first proof-of-concept that visually-indistinguishable training attacks can be executed on otherwise highly-accurate neural networks.

For a target test image z_{test} , we can construct for each training image z_i an adversarial perturbation $\delta_i = \text{clip}(\text{sign}(\mathcal{I}_{\text{pert,loss}}(z_i, z_{\text{test}})))$, which makes a visually-imperceptible change to z_i (each pixel is perturbed by at most 1 and clipped to $[0, 255]$). This is a training-set analogue of the fast gradient sign method used by (Goodfellow et al., 2015) for test-set attacks.

We tested these adversarial training perturbations on the same Inception network on dogs vs. fish from Section 5.1, choosing this pair of animals to provide a stark contrast between the classes. As before, we froze all but the top layer for training; note that $\mathcal{I}_{\text{pert,loss}}$ still involves differentiating through the entire network. We targeted the test image in Fig 5. In Fig 5a, we plot the changes in test loss expected from each δ_i : most perturbations had little effect, but a few caused sharp increases in test loss. We applied the δ_i with the largest expected effect and retrained the model. Sur-

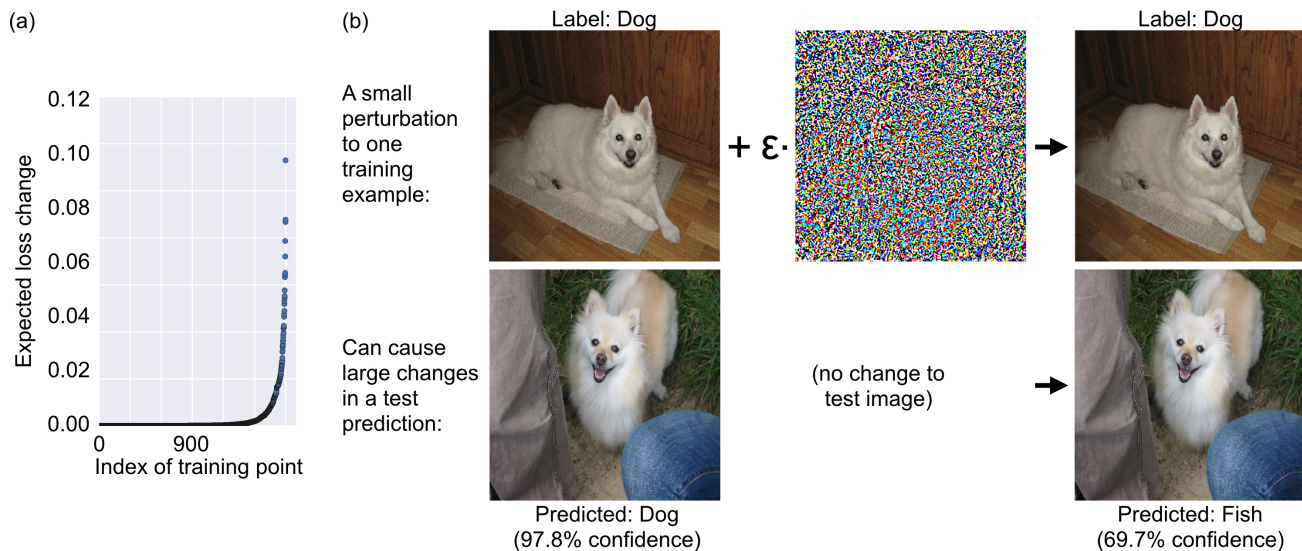


Figure 5. **Training-set attacks.** (a) We plot the change in loss expected from an attack on each training point in sorted order. A small number of training examples have large expected changes. (b) A small perturbation on one training example flipped the test prediction.

prisingly, this small change to just 1 out of 1,800 training images flipped the prediction on the test image (Fig 5b).

Other test images were also vulnerable. For each z_{test} , we computed δ_i for each training example i and greedily applied them in descending order of their expected effect. Originally, the model correctly classified 592 / 600 test images. Out of these 592, 20 predictions could be flipped by perturbing only 1 training image per prediction (choosing a different training example for each test image). 54% of the test predictions could be flipped if we allowed perturbations on 18 training images (1% of train data, again with a different 18 training images for each test image), and 87% of the test predictions could be flipped with perturbations on 36 training images (2% of train data) per test image.

This training-set attack extends to a broader class of targets (e.g., increasing test loss on an entire class) using the same approach. One could also increase its effectiveness by iterating gradient steps, resulting in larger perturbations. We note that this attack is mathematically similar to the gradient-based dataset poisoning attacks explored by Biggio et al. (2012); Mei & Zhu (2015b) and others in the context of different models; we elaborate on this connection in section 6. Biggio et al. (2012) constructed a dataset poisoning attack against a linear SVM on a two-class MNIST task, but had to modify the training points in an obviously distinguishable way to be effective. Measuring the magnitude of $\mathcal{I}_{\text{pert,loss}}$ gives model developers a way of quantifying how vulnerable their models are to training-set perturbations.

5.3. Debugging domain mismatch

Domain mismatch — where the training distribution does not match the test distribution — can cause models with high training accuracy to do poorly on test data (Ben-David et al., 2010). We show that influence functions can identify the training examples most responsible for the errors, helping model developers to pinpoint a domain mismatch.

As a case study, we predicted whether a patient would be readmitted to a hospital. Domain mismatches are common in biomedical data; for example, different hospitals can serve very different populations, and readmission models trained on one population can do poorly on another (Kansagara et al., 2011). We used logistic regression to predict readmission with a balanced training dataset of 20K diabetic patients from 100+ US hospitals, each represented by 127 features (Strack et al., 2014).⁷

3 out of the 24 children under age 10 in this dataset were re-admitted. To induce a domain mismatch, we filtered out 20 children who were not re-admitted, leaving 3 out of 4 re-admitted. This caused the model to wrongly classify many children in the test set. Our aim is to identify the 4 children in the training set as being “responsible” for these errors.

As a baseline, we looked at the learned parameters $\hat{\theta}$ to see if the indicator variable for being a child was obviously different, but 11/127 features had a larger coefficient, e.g., whether the patient was referred to a different hospital.

⁷Hospital readmission was defined as whether a patient would be readmitted within the next 30 days. Features were demographic (e.g., age, race, gender), administrative (e.g., length of hospital stay), or medical (e.g., test results).

Picking a random child z_{test} that the model got wrong, we calculated $-\mathcal{I}_{\text{up,loss}}(z_i, z_{\text{test}})$ for each training point z_i . This clearly highlighted the 4 training children, each of whom was more than 100 times as influential as the next most influential examples. The 1 child in the training set who was not readmitted had a very positive influence, while the other 3 had very negative influences. Calculating $\mathcal{I}_{\text{pert,loss}}$ on these 4 children showed that a change in the ‘child’ indicator variable had by far the largest effect on $\mathcal{I}_{\text{up,loss}}$.

5.4. Fixing mislabeled examples

Labels in the real world are often noisy, especially if crowd-sourced (Fréney & Verleysen, 2014), and can even be adversarially corrupted, as in section 5.2. Even if a human expert could recognize wrongly labeled examples, it is impossible in many applications to manually review all of the training data. We show that influence functions can help human experts prioritize their attention, allowing them to inspect only the examples that actually matter.

The key idea is to flag the training points that exert the most influence on the model. Because we do not have access to the test set, we measure the influence of z_i with $-\frac{1}{n}\mathcal{I}_{\text{up,loss}}(z_i, z_i)$, which approximates the leave-one-out error incurred on z_i if we remove z_i from the training set.

Our case study is email spam classification, which relies on user-provided labels and is also vulnerable to adversarial attack (Biggio et al., 2011).⁸ We flipped the labels of a random 10% of the training data and then simulated manually inspecting a fraction of the training points, correcting them if they had been flipped. Using influence functions to prioritize the training points to inspect allowed us to repair the dataset (Fig 6, blue) without checking too many points, outperforming the baselines of checking points with the highest train loss (Fig 6, green) or at random (Fig 6, red). No method had access to the test data.

6. Related work

The use of influence-based diagnostics originated in statistics in the 70s and 80s, driven by seminal papers by Cook and others (Cook, 1977; Cook & Weisberg, 1980; 1982), though similar ideas appeared even earlier in other forms, e.g., the infinitesimal jackknife (Jaekel, 1972). Earlier work focused on removing training points from linear models, with later work extending this to more general models and a wider variety of perturbations (Cook, 1986; Thomas & Cook, 1990; Chatterjee & Hadi, 1986; Wei et al., 1998). Most of this prior work focused on experiments with small datasets, e.g., $n = 24$ and $p = 10$ in Cook & Weisberg

⁸We divided the Enron1 spam dataset (Metsis et al., 2006) into training ($n = 4147$) and test ($n = 1035$) sets, training logistic regression on top of a bag-of-words representation.

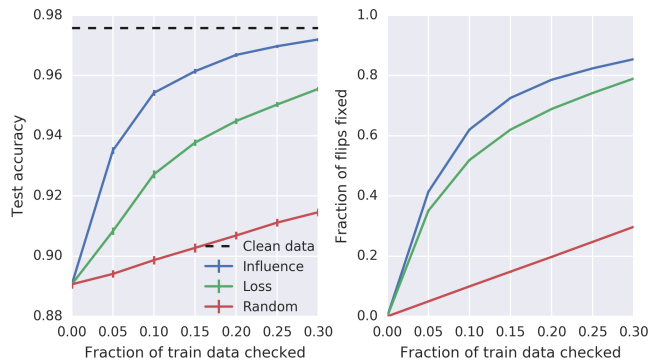


Figure 6. **Fixing mislabeled examples.** Plots of how test accuracy (left) and the fraction of flipped data detected (right) change with the fraction of train data checked, using different algorithms for picking points to inspect. Error bars show the standard deviation across 40 different random subsets of flipped labels; error bars on the right are too small to be seen.

(1980), with special attention therefore paid to exact solutions, or if not possible, characterizations of the error terms.

To the best of our knowledge, influence functions have not been used much in the ML literature, with some exceptions. Christmann & Steinwart (2004); Debruyne et al. (2008); Liu et al. (2014) use influence functions to study model robustness and to do fast cross-validation in kernel methods. Wojnowicz et al. (2016) uses matrix sketching to estimate Cook’s distance, which is closely related to influence; they focus on prioritizing training points for human attention and derive methods specific to generalized linear models.

As noted in section 5.2, our training-set attack is mathematically similar to an approach first explored by Biggio et al. (2012) in the context of SVMs, with follow-up work extending the framework and applying it to linear and logistic regression (Mei & Zhu, 2015b), topic modeling (Mei & Zhu, 2015a), and collaborative filtering (Li et al., 2016a). These papers derived the attack directly from the KKT conditions without considering influence functions, though for continuous data the end result is equivalent to iterating $\mathcal{I}_{\text{pert,loss}}$. Influence functions additionally allow us to consider attacks that change discrete data (section 2.2) and potentially models that are not convex or differentiable (sections 4.2, 4.3), though more work needs to be done to test the effectiveness of those attacks. Our work merges elements of this approach with the work of Goodfellow et al. (2015) and others on visually-imperceptible, adversarial test-set attacks in neural networks: we cast the dataset poisoning attack in the influence function framework and apply it in a larger-scale, neural network setting, creating a visually-imperceptible attack on the training set.

In contrast to training-set attacks, Cadamuro et al. (2016) consider the task of taking an incorrect test prediction and

finding a small subset of training data such that changing the labels on this subset makes the prediction correct. They provide a solution for OLS and Gaussian process models when the labels are continuous. Our work with influence functions allow us to solve this problem in a much larger range of models and in datasets with discrete labels.

7. Discussion

We have discussed a variety of applications, from detecting training-set vulnerabilities to debugging models and fixing datasets. Underlying each of these applications is a common tool, influence functions, which are based on a simple idea — we can better understand model behavior by looking at how it was derived from its training data.

At their core, influence functions measure the effect of local changes: what happens when we upweight a point by an infinitesimally-small ϵ ? This locality allows us to derive efficient closed-form estimates, and as we show, they can be surprisingly effective. However, we might want to ask about more global changes, e.g., how does the set of all patients from this hospital affect the model? Since the accuracy of influence functions is based on the model not changing too much, how to tackle this is an open question.

It seems inevitable that high-performing, complex, black-box models will become increasingly prevalent and important. We hope that the approach presented here — of looking at the training data through the lens of the model — will become a standard part of the toolkit of developing, understanding, and diagnosing these models.

A. Deriving $\mathcal{I}_{\text{up, params}}$

Here, we give a standard derivation of the influence function $\mathcal{I}_{\text{up, params}}$ in the context of M-estimation; a much more thorough treatment can be found in (van der Vaart, 1998) and other statistics textbooks.

As a reminder, our setting is unconstrained empirical risk minimization. We assume that we are given parameters $\hat{\theta}$ that are the global minimum of the empirical risk $\frac{1}{n} \sum_{i=1}^n L(z_i, \theta)$. We further assume that the empirical risk is twice-differentiable and strongly convex in θ in a local neighborhood around $\hat{\theta}$, i.e., $H_{\hat{\theta}} \triangleq \frac{1}{n} \sum_{i=1}^n \nabla_{\theta}^2 L(z_i, \hat{\theta})$ exists and is positive definite. This guarantees the existence of $H_{\hat{\theta}}^{-1}$, which we will use in the subsequent derivation.

Our goal is to find $\hat{\theta}_{\epsilon, z}$, the model parameters that result from upweighting a training point z by an infinitesimal ϵ . This perturbation results in a modified empirical risk $\tilde{R}(\theta, \epsilon, z) \triangleq (1 - \epsilon) \frac{1}{n} \sum_{i=1}^n L(z_i, \theta) + \epsilon L(z, \theta)$, with $\hat{\theta}_{\epsilon, z} \triangleq \arg \min_{\theta} \tilde{R}(\theta, \epsilon, z)$.

At a high level, our strategy will be as follows: since ϵ is

small and the empirical risk is strongly convex around $\hat{\theta}$, we can assume that $\hat{\theta}_{\epsilon, z}$ is close to $\hat{\theta}$. We can therefore write $\tilde{R}(\hat{\theta}_{\epsilon, z}, \epsilon, z)$ in terms of $\hat{\theta}$ by taking Taylor expansions of L around $\hat{\theta}$; minimizing this expanded version of \tilde{R} will give us the desired formula for $\mathcal{I}_{\text{up, params}}$.

For convenience, define $\Delta = \theta - \hat{\theta}$. The second-order Taylor expansion of L around $\hat{\theta}$ at a training point z_i is given by

$$L(z_i, \theta) = L(z_i, \hat{\theta}) + \nabla_{\theta} L(z_i, \hat{\theta})^{\top} \Delta + \frac{1}{2} \Delta^{\top} \nabla_{\theta}^2 L(z_i, \hat{\theta}) \Delta + o(\|\Delta\|_2^2). \quad (6)$$

Since $\Delta_{\epsilon, z} \triangleq \hat{\theta}_{\epsilon, z} - \hat{\theta}$ is small, we can restrict our attention to values of θ that are close to $\hat{\theta}$ and ignore the $o(\|\Delta\|_2^2)$ term. Substituting this expansion into \tilde{R} gives us:

$$\begin{aligned} \tilde{R}(\theta, \epsilon, z) &= (1 - \epsilon) \frac{1}{n} \sum_{i=1}^n L(z_i, \theta) + \epsilon L(z, \theta) \\ &\approx (1 - \epsilon) \frac{1}{n} \sum_{i=1}^n L(z_i, \hat{\theta}) + \epsilon L(z, \hat{\theta}) \\ &\quad + (1 - \epsilon) \frac{1}{n} \sum_{i=1}^n \nabla_{\theta} L(z_i, \hat{\theta})^{\top} \Delta + \epsilon \nabla_{\theta} L(z, \hat{\theta})^{\top} \Delta \\ &\quad + \frac{1 - \epsilon}{2n} \sum_{i=1}^n \Delta^{\top} \nabla_{\theta}^2 L(z_i, \hat{\theta}) \Delta + \frac{\epsilon}{2} \Delta^{\top} \nabla_{\theta}^2 L(z, \hat{\theta}) \Delta, \end{aligned} \quad (7)$$

where the approximation comes from discarding the $o(\|\Delta\|_2^2)$ term.

Now, since $\hat{\theta}_{\epsilon, z}$ minimizes $\tilde{R}(\theta, \epsilon, z)$, we know that $\frac{d}{d\theta} \tilde{R}(\hat{\theta}_{\epsilon, z}, \epsilon, z) = 0$. Applying this to eqn 7 gives us

$$\Delta_{\epsilon, z} = - \left[\begin{aligned} &(1 - \epsilon) \frac{1}{n} \sum_{i=1}^n \nabla_{\theta}^2 L(z_i, \hat{\theta}) + \epsilon \nabla_{\theta}^2 L(z, \hat{\theta}) \\ &(1 - \epsilon) \frac{1}{n} \sum_{i=1}^n \nabla_{\theta} L(z_i, \hat{\theta}) + \epsilon \nabla_{\theta} L(z, \hat{\theta}) \end{aligned} \right]^{-1}. \quad (8)$$

We can simplify this by using the fact that the original $\hat{\theta}$ satisfies the optimality condition $\sum_{i=1}^n \nabla_{\theta} L(z_i, \hat{\theta}) = 0$, since $\hat{\theta}$ is a local minimum of the empirical risk. Furthermore, for small ϵ and any positive-definite matrix A , $(I + \epsilon A)^{-1} = I - \epsilon A + o(\epsilon)$. Discarding the $o(\epsilon)$ term, we thus have

$$\Delta_{\epsilon, z} \approx - \left[\frac{1}{n} \sum_{i=1}^n \nabla_{\theta}^2 L(z_i, \hat{\theta}) \right]^{-1} \epsilon \nabla_{\theta} L(z, \hat{\theta}) + o(\epsilon). \quad (9)$$

Finally, differentiating this w.r.t. ϵ yields the desired result:

$$\begin{aligned} \left. \frac{d\hat{\theta}_{\epsilon,z}}{d\epsilon} \right|_{\epsilon=0} &= \left. \frac{d\Delta_{\epsilon,z}}{d\epsilon} \right|_{\epsilon=0} \\ &= - \left[\frac{1}{n} \sum_{i=1}^n \nabla_{\theta}^2 L(z_i, \hat{\theta}) \right]^{-1} \nabla_{\theta} L(z, \hat{\theta}) \\ &= -H_{\hat{\theta}}^{-1} \nabla_{\theta} L(z, \hat{\theta}) \\ &= \mathcal{I}_{\text{up,params}}(z). \end{aligned} \quad (10)$$

Because $H_{\hat{\theta}} \succ 0$ by assumption, its inverse exists. Without this assumption (e.g., $\hat{\theta}$ is still the global minimum but $H_{\hat{\theta}}$ has eigenvalues that are zero), our second-order Taylor expansion would fail and we would need to go to higher-order derivatives of L at $\hat{\theta}$. One way to overcome this is by adding a small damping term λI to $H_{\hat{\theta}}$, which has the effect of regularizing $\hat{\theta}_{\epsilon,z}$ so that it stays close to $\hat{\theta}$.

If the empirical risk is non-convex in θ , then $\hat{\theta}$ might not even be the global minimum. We study this in section 4.2 and appendix B.

B. Influence at non-convergence

Consider a training point z . When the model parameters $\tilde{\theta}$ are close to but not at a local minimum, $\mathcal{I}_{\text{up,params}}(z)$ is correlated with the change in parameters after upweighting z and then taking a single Newton step from $\tilde{\theta}$. The high-level idea is that even though the gradient of the empirical risk at $\tilde{\theta}$ is not 0, the Newton step from $\tilde{\theta}$ can be decomposed into a component following the existing gradient (which does not depend on the choice of z) and a second component responding to the upweighted z (which $\mathcal{I}_{\text{up,params}}(z)$ tracks).

Let $c \triangleq \frac{1}{n} \sum_{i=1}^n \nabla_{\theta} L(z_i, \tilde{\theta})$ be the gradient of the empirical risk at $\tilde{\theta}$; since $\tilde{\theta}$ is not a local minimum, $c \neq 0$. After upweighting z by ϵ , the gradient at $\tilde{\theta}$ goes from $c \mapsto (1 - \epsilon)c + \epsilon \nabla_{\theta} L(z, \tilde{\theta})$, and the empirical Hessian goes from $H_{\tilde{\theta}} \mapsto (1 - \epsilon)H_{\tilde{\theta}} + \epsilon \nabla_{\theta}^2 L(z, \tilde{\theta})$. A Newton step from $\tilde{\theta}$ therefore changes the parameters by:

$$N_{\epsilon,z} \triangleq - \left[(1 - \epsilon)H_{\tilde{\theta}} + \epsilon \nabla_{\theta}^2 L(z, \tilde{\theta}) \right]^{-1} \left[(1 - \epsilon)c + \epsilon \nabla_{\theta} L(z, \tilde{\theta}) \right]. \quad (11)$$

If $c \gg \epsilon \nabla_{\theta} L(z, \tilde{\theta})$, i.e., the model is far from convergence and still has a large gradient, then $N_{\epsilon,z} \approx -H_{\tilde{\theta}}^{-1}c$. In this case, the effect of downweighting z is swamped by c .

However, if c is on the same order as $\epsilon \nabla_{\theta} L(z, \tilde{\theta})$, then by ignoring terms in ϵc , ϵ^2 , and higher, we get $N_{\epsilon,z} \approx -H_{\tilde{\theta}}^{-1} \left(c + \epsilon \nabla_{\theta} L(z, \tilde{\theta}) \right)$. Since $\mathcal{I}_{\text{up,params}}(z) =$

$-H_{\tilde{\theta}}^{-1} \nabla_{\theta} L(z, \tilde{\theta})$, it is a scaled multiple of $N_{\epsilon,z}$ plus a constant $-H_{\tilde{\theta}}^{-1}c$.

Acknowledgements

We thank Jacob Steinhardt, Zhenghao Chen, and Hongseok Namkoong for helpful discussions and comments. This work was supported by a Future of Life Research Award and a Microsoft Research Faculty Fellowship.

References

- Abadi, M., Agarwal, A., Barham, P., Brevdo, E., Chen, Z., Citro, C., Corrado, G. S., Davis, A., Dean, J., Devin, M., Ghemawat, S., Goodfellow, I. J., Harp, A., Irving, G., Isard, M., Jia, Y., Józefowicz, R., Kaiser, L., Kudlur, M., Levenberg, J., Mané, D., Monga, R., Moore, S., Murray, D. G., Olah, C., Schuster, M., Shlens, J., Steiner, B., Sutskever, I., Talwar, K., Tucker, P. A., Vanhoucke, V., Vasudevan, V., Viégas, F. B., Vinyals, O., Warden, P., Wattenberg, M., Wicke, M., Yu, Y., and Zheng, X. Tensorflow: Large-scale machine learning on heterogeneous distributed systems. *arXiv preprint arXiv:1603.04467*, 2015.
- Adler, P., Falk, C., Friedler, S. A., Rybeck, G., Scheidegger, C., Smith, B., and Venkatasubramanian, S. Auditing black-box models for indirect influence. *arXiv preprint arXiv:1602.07043*, 2016.
- Agarwal, N., Bullins, B., and Hazan, E. Second order stochastic optimization in linear time. *arXiv preprint arXiv:1602.03943*, 2016.
- Amershi, S., Chickering, M., Drucker, S. M., Lee, B., Simard, P., and Suh, J. Modeltracker: Redesigning performance analysis tools for machine learning. In *Conference on Human Factors in Computing Systems (CHI)*, pp. 337–346, 2015.
- Ben-David, S., Blitzer, J., Crammer, K., Kulesza, A., Pereira, F., and Vaughan, J. W. A theory of learning from different domains. *Machine Learning*, 79(1):151–175, 2010.
- Biggio, B., Nelson, B., and Laskov, P. Support vector machines under adversarial label noise. *ACML*, 20:97–112, 2011.
- Biggio, B., Nelson, B., and Laskov, P. Poisoning attacks against support vector machines. In *International Conference on Machine Learning (ICML)*, pp. 1467–1474, 2012.
- Cadamuro, G., Gilad-Bachrach, R., and Zhu, X. Debugging machine learning models. In *ICML Workshop on Reliable Machine Learning in the Wild*, 2016.

- Chatterjee, S. and Hadi, A. S. Influential observations, high leverage points, and outliers in linear regression. *Statistical Science*, pp. 379–393, 1986.
- Chollet, F. *Keras*, 2015.
- Christmann, A. and Steinwart, I. On robustness properties of convex risk minimization methods for pattern recognition. *Journal of Machine Learning Research (JMLR)*, 5(0):1007–1034, 2004.
- Cook, R. D. Detection of influential observation in linear regression. *Technometrics*, 19:15–18, 1977.
- Cook, R. D. Assessment of local influence. *Journal of the Royal Statistical Society. Series B (Methodological)*, pp. 133–169, 1986.
- Cook, R. D. and Weisberg, S. Characterizations of an empirical influence function for detecting influential cases in regression. *Technometrics*, 22:495–508, 1980.
- Cook, R. D. and Weisberg, S. *Residuals and influence in regression*. New York: Chapman and Hall, 1982.
- Datta, A., Sen, S., and Zick, Y. Algorithmic transparency via quantitative input influence: Theory and experiments with learning systems. In *Security and Privacy (SP), 2016 IEEE Symposium on*, pp. 598–617, 2016.
- Debruyne, M., Hubert, M., and Suykens, J. A. Model selection in kernel based regression using the influence function. *Journal of Machine Learning Research (JMLR)*, 9(0):2377–2400, 2008.
- Donahue, J., Jia, Y., Vinyals, O., Hoffman, J., Zhang, N., Tzeng, E., and Darrell, T. Decaf: A deep convolutional activation feature for generic visual recognition. In *International Conference on Machine Learning (ICML)*, volume 32, pp. 647–655, 2014.
- Frénay, B. and Verleysen, M. Classification in the presence of label noise: a survey. *IEEE Transactions on Neural Networks and Learning Systems*, 25:845–869, 2014.
- Goodfellow, I. J., Shlens, J., and Szegedy, C. Explaining and harnessing adversarial examples. In *International Conference on Learning Representations (ICLR)*, 2015.
- Goodman, B. and Flaxman, S. European union regulations on algorithmic decision-making and a “right to explanation”. *arXiv preprint arXiv:1606.08813*, 2016.
- Huang, L., Joseph, A. D., Nelson, B., Rubinstein, B. I., and Tygar, J. Adversarial machine learning. In *Proceedings of the 4th ACM workshop on Security and artificial intelligence*, pp. 43–58, 2011.
- Jaeckel, L. A. The infinitesimal jackknife. *Unpublished memorandum, Bell Telephone Laboratories, Murray Hill, NJ*, 1972.
- Kansagara, D., Englander, H., Salanitro, A., Kagen, D., Theobald, C., Freeman, M., and Kripalani, S. Risk prediction models for hospital readmission: a systematic review. *JAMA*, 306(15):1688–1698, 2011.
- Kingma, D. and Ba, J. Adam: A method for stochastic optimization. *arXiv preprint arXiv:1412.6980*, 2014.
- Krizhevsky, A., Sutskever, I., and Hinton, G. E. Imagenet classification with deep convolutional neural networks. In *Advances in Neural Information Processing Systems (NIPS)*, pp. 1097–1105, 2012.
- LeCun, Y., Bottou, L., Bengio, Y., and Haffner, P. Gradient-based learning applied to document recognition. *Proceedings of the IEEE*, 86(11):2278–2324, 1998.
- Li, B., Wang, Y., Singh, A., and Vorobeychik, Y. Data poisoning attacks on factorization-based collaborative filtering. In *Advances in Neural Information Processing Systems (NIPS)*, pp. 1885–1893, 2016a.
- Li, J., Monroe, W., and Jurafsky, D. Understanding neural networks through representation erasure. *arXiv preprint arXiv:1612.08220*, 2016b.
- Liu, D. C. and Nocedal, J. On the limited memory BFGS method for large scale optimization. *Mathematical Programming*, 45(1):503–528, 1989.
- Liu, Y., Jiang, S., and Liao, S. Efficient approximation of cross-validation for kernel methods using Bouligand influence function. In *International Conference on Machine Learning (ICML)*, pp. 324–332, 2014.
- Martens, J. Deep learning via hessian-free optimization. In *International Conference on Machine Learning (ICML)*, pp. 735–742, 2010.
- Mei, S. and Zhu, X. The security of latent Dirichlet allocation. In *Artificial Intelligence and Statistics (AISTATS)*, 2015a.
- Mei, S. and Zhu, X. Using machine teaching to identify optimal training-set attacks on machine learners. In *Association for the Advancement of Artificial Intelligence (AAAI)*, 2015b.
- Metsis, V., Androutsopoulos, I., and Paliouras, G. Spam filtering with naive bayes-which naive bayes? In *CEAS*, volume 17, pp. 28–69, 2006.
- Pearlmutter, B. A. Fast exact multiplication by the hessian. *Neural Computation*, 6(1):147–160, 1994.

- Ribeiro, M. T., Singh, S., and Guestrin, C. "why should I trust you?": Explaining the predictions of any classifier. In *International Conference on Knowledge Discovery and Data Mining (KDD)*, 2016.
- Russakovsky, O., Deng, J., Su, H., Krause, J., Satheesh, S., Ma, S., Huang, Z., Karpathy, A., Khosla, A., Bernstein, M., et al. ImageNet large scale visual recognition challenge. *International Journal of Computer Vision*, 115(3): 211–252, 2015.
- Shrikumar, A., Greenside, P., Shcherbina, A., and Kundaje, A. Not just a black box: Learning important features through propagating activation differences. *arXiv preprint arXiv:1605.01713*, 2016.
- Simonyan, K., Vedaldi, A., and Zisserman, A. Deep inside convolutional networks: Visualising image classification models and saliency maps. *arXiv preprint arXiv:1312.6034*, 2013.
- Springenberg, J. T., Dosovitskiy, A., Brox, T., and Riedmiller, M. Striving for simplicity: The all convolutional net. *arXiv preprint arXiv:1412.6806*, 2014.
- Strack, B., DeShazo, J. P., Gennings, C., Olmo, J. L., Ventura, S., Cios, K. J., and Clore, J. N. Impact of HbA1c measurement on hospital readmission rates: analysis of 70,000 clinical database patient records. *BioMed Research International*, 2014, 2014.
- Szegedy, C., Vanhoucke, V., Ioffe, S., Shlens, J., and Wojna, Z. Rethinking the Inception architecture for computer vision. In *Computer Vision and Pattern Recognition (CVPR)*, pp. 2818–2826, 2016.
- Theano D. Team. Theano: A Python framework for fast computation of mathematical expressions. *arXiv preprint arXiv:1605.02688*, 2016.
- Thomas, W. and Cook, R. D. Assessing influence on predictions from generalized linear models. *Technometrics*, 32(1):59–65, 1990.
- van der Vaart, A. W. *Asymptotic statistics*. Cambridge University Press, 1998.
- Wei, B., Hu, Y., and Fung, W. Generalized leverage and its applications. *Scandinavian Journal of Statistics*, 25: 25–37, 1998.
- Wojnowicz, M., Cruz, B., Zhao, X., Wallace, B., Wolff, M., Luan, J., and Crable, C. "Influence sketching": Finding influential samples in large-scale regressions. *arXiv preprint arXiv:1611.05923*, 2016.